Dynamics of Enhanced Tracer Diffusion in Suspensions of Eukaryotic Microorganisms

Kyriacos C. Leptos[1], Jeffrey S. Guasto[2], J.P. Gollub[1,2], Adriana I. Pesci[1] and Raymond E. Goldstein[1]
[1]*Department of Applied Mathematics and Theoretical Physics, University of Cambridge, Wilberforce Road, Cambridge CB3 0WA, UK and*
[2]*Department of Physics, Haverford College, Haverford, PA 19041*
(Dated: June 25, 2009)

In contexts such as suspension feeding in marine ecologies there is an interplay between Brownian motion of non-motile particles and their advection by flows from swimming microorganisms. As a laboratory realization, we study passive tracers in suspensions of eukaryotic swimmers, the alga *Chlamydomonas reinhardtii*. While the cells behave ballistically over short intervals, the tracers behave diffusively, with a time-dependent but self-similar probability distribution function of displacements consisting of a Gaussian core and robust exponential tails. We emphasize the role of flagellar beating in creating oscillatory flows that exceed Brownian motion far from each swimmer.

PACS numbers: 87.17.Jj, 05.40.-a, 47.63.Gd, 87.23.-n

For many of the microscopic organisms in marine and lake environments the process of feeding involves an interplay between diffusion of target particles and their advection in the flow field of the swimmers [1–4]. When the particles are large and discrete, and hence display little random motion, the rate of interception is determined primarily by their size and the details of fluid streamlines around the swimmers, while for molecular species, the rate of uptake involves the formation of boundary layers characteristic of high Péclet number flows [3, 5, 6]. As the concentration of swimmers increases, the greater frequency of encounter of suspended particles with the swimmer flow fields will inevitably lead to enhanced transport of the particles themselves.

At high concentrations there is now ample evidence from studies of bacterial systems [7–10] that collective behavior can emerge, consisting of large-scale vortices and jets which dramatically enhance tracer particle transport and fluid mixing. Such mixing may have microfluidic applications [11, 12]. While there has been significant progress in understanding collective behavior [13–16], the fundamental problem of understanding enhanced tracer diffusion induced by swimmers has remained largely unsolved, even in the dilute limit.

One appealing point of view [7, 17] is that the sea of swimming organisms constitutes an effective"thermal bath," analogous to the multitudes of molecules responsible for Brownian motion, where each encounter of a tracer particle with a swimmer provides a random kick. In conventional Brownian motion, *e.g.* with micron-size particles in water, there is an enormous separation of time scales between the duration of molecular collisions and the observed particle motion, which justifies the picture of a Markov process. In contrast, in a suspension of microorganisms it is possible to resolve the encounters with tracer particles, and the dynamical problem involves correlated *advective trajectories* in the presence of true Brownian noise. This problem is reminiscent of passive scalar advection in turbulent flows [18], where the probability distribution functions (PDF) of tracer displacements become strongly non-Gaussian.

Here we report an advance in the study of tracer statistics in suspensions of swimmers based on two key features. First, we use the alga *Chlamydomonas reinhardtii* [19], a biflagellated model eukaryote in the study of flagella and photosynthesis. Relative to the bacteria investigated previously [7–10] (*E. coli*, *B. subtilis*) *Chlamydomonas* has several key features which will greatly simplify the theoretical interpretation of our results; it has a nearly spherical shape, is sufficiently large (a radius $R \sim 5$ μm) that its motion is not subject to substantial rotational diffusion, and as its two $10-12$ μm long flagella beat in a synchronized "breast stroke" pattern at $50-60$ Hz, it displays long periods of nearly straight-line motion. Second, we characterize in detail the time-dependent PDF of tracer displacements, and find clear systematic deviations from Gaussianity, in the form of an exponential tail whose amplitude grows with swimmer concentration. Despite this complex form, the PDFs exhibit self-similarity under a diffusive scaling. Some theoretical considerations that may be important in a microscopic theory of these results are suggested.

Microscopy of *Chlamydomonas* suspensions was carried out on a Nikon TE2000-U inverted fluorescence microscope inside chambers fabricated from polydimethylsiloxane (PDMS), 1 cm in diameter and 1.5 mm deep. After casting, each cavity was etched in an oxygen plasma (Femto, Diener Electronic) and bonded to a PDMS-spin-coated cover slip. Both the interior of the chambers and the fluorescent particles were pacified using a 5% (w/v) solution of bovine serum albumin to prevent the protein in the flagella from adhering to them [20]. *Chlamydomonas reinhardtii* (UTEX 89) was grown axenically in Tris-Acetate-Phosphate (TAP) medium [19], on an orbital shaker (300 rpm) in a diurnal growth chamber (KBW400, Binder). The daily cycle was 16 h of cool

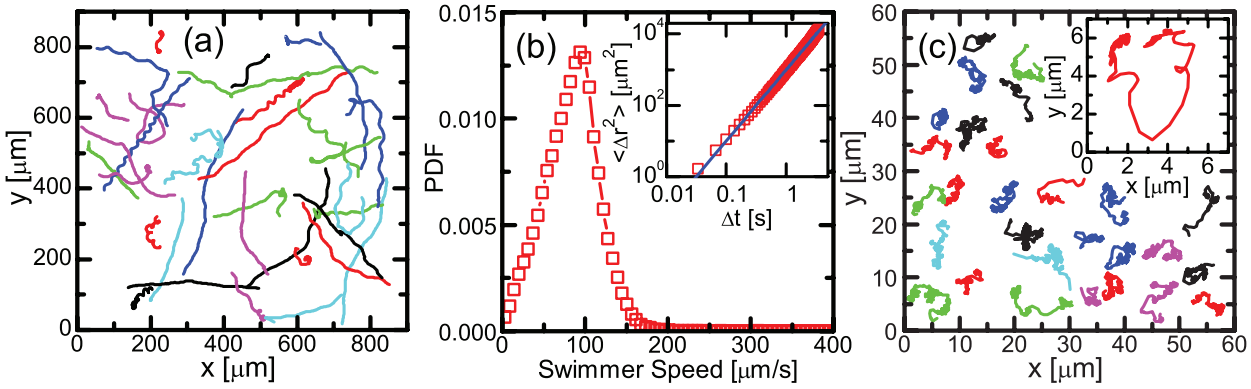

FIG. 1: (Color online) Swimming cells and tracer particles. (a) *Chlamydomonas* trajectories over an interval of $\sim$ 1s. (b) Probability distribution of swimming speed and (inset) mean squared displacement of swimmers in the imaging plane. The line $\langle \Delta r^2 \rangle \sim t^2$ shows the motion to be ballistic for intervals up to several s. (c) Trajectories of 2.0 μm microspheres observed at 50 fps. Inset shows a loopy tracer trajectory, sampled at 500 fps, induced by a swimmer passing within about 8 μm.

white light ($\sim$ 80 μmol photons/m^{2}s) at 28 °C, and 8 h in the dark at 26 °C. For concentrations $> 10^6$ cells/cm^3, cells were concentrated from exponentially growing cultures by centrifugation in tubes at $1100 \times g$ and addition of fresh TAP to the cell pellet. The tubes were then placed in the diurnal chamber for at least 1 h to allow the cells to recuperate. All cell concentrations were measured using a haemocytometer [21]. Fluorescent microspheres (yellow-green, Invitrogen F8827; radius $a = 1$ μm,) were added to obtain a final concentration of $\sim$ 250 ppm (w/v). Each sample was transferred to a separate PDMS observation chamber, taking care to avoid excessive shear that might damage the flagella. Movies of cells and of tracer particles were recorded with a high-speed video camera (Fastcam SA-3, Photron) at up to 500 fps to resolve motion induced by flagellar beating. Tracers were observed at $\times$40 with epifluorescence illumination (Pantachrome, Till Photonics) in a plane $\sim$ 100 μm above the chamber bottom. Cell and particle trajectories were extracted from recordings with a predictive particle tracking algorithm [22].

A relatively dilute suspension of cells in growth medium was first studied at $\times$20 magnification with bright-field illumination, using a red longpass filter ($\lambda >$ 620 nm) to prevent phototaxis. While cell trajectories have been studied previously [23], it is important to characterize them *in situ* along with the tracer dynamics. The representative sample in Fig. 1a illustrates a broad spectrum of trajectories including helical paths of variable pitch – the well-known spinning of the body around the trajectory midline. The cell velocity distribution in the imaging plane (Fig. 1b) shows a peak at $\sim$ 100 μm/s. There is some out-of-plane motion that is not imaged, so the 3D distribution is likely even sharper. The distribution is consistent with swimming at approximately constant speed in random directions. Indeed, while many trajectories' centerlines are gently curved, sharp turns are only observed on longer intervals [24]. A statistical analysis of cell displacements along an arbitrary axis in the imaging plane shows *ballistic* behavior (Fig. 2b, inset) up to several seconds. Tracer trajectories (Fig. 1c and inset) involve both Brownian components and large jumps induced by flows from the swimmers. Higher magnification (inset) shows that these advective motions are loops due to flagellar beating.

For each volume fraction ϕ of *Chlamydomonas* the PDF of tracer displacements $P(\Delta x, \Delta t)$ along an arbitrary direction was calculated for a number of increasing time intervals Δt. The intervals used were well within the ballistic regime of the swimmers (Fig. 1b), and an order of magnitude smaller than the the mean time between sharp turns measured in three-dimensional tracking experiments [24]. Figure 2a shows the PDF at a fixed interval ($\Delta t = 0.12$ s) for increasing ϕ. Without swimmers, the distribution is accurately fitted by a Gaussian whose width is determined by a diffusion constant $D_0 = 0.28$ μm^2/s, consistent with the Stokes-Einstein value.

In the presence of swimmers, there are two changes to the distributions. First, exponential tails appear in the PDFs, the magnitude of which grows with increasing concentration of swimmers. Second, the Gaussian core broadens significantly. For all volume fractions ϕ and time intervals Δt that we have studied the distributions $P(\Delta x, \Delta t)$ can be fitted accurately to a weighted sum of Gaussian and exponential (Laplace) distributions,

$$P(\Delta x, \Delta t) = \frac{1-f}{(2\pi\delta_g^2)^{1/2}} \mathrm{e}^{-(\Delta x)^2/2\delta_g^2} + \frac{f}{2\delta_e} \mathrm{e}^{-|\Delta x|/\delta_e} \ . \quad (1)$$

There are three parameters: the standard deviation $\delta_g(\Delta t, \phi)$ of the Gaussian distribution, the decay length $\delta_e(\Delta t, \phi)$ of the Laplace distribution, and the fraction of time $f(\phi)$ during which the displacements are enhanced by advection. We find that the lengths both exhibit diffusive growth, with $\delta_g \simeq A_g \Delta t^{1/2}$ and $\delta_e \simeq A_e \Delta t^{1/2}$. This

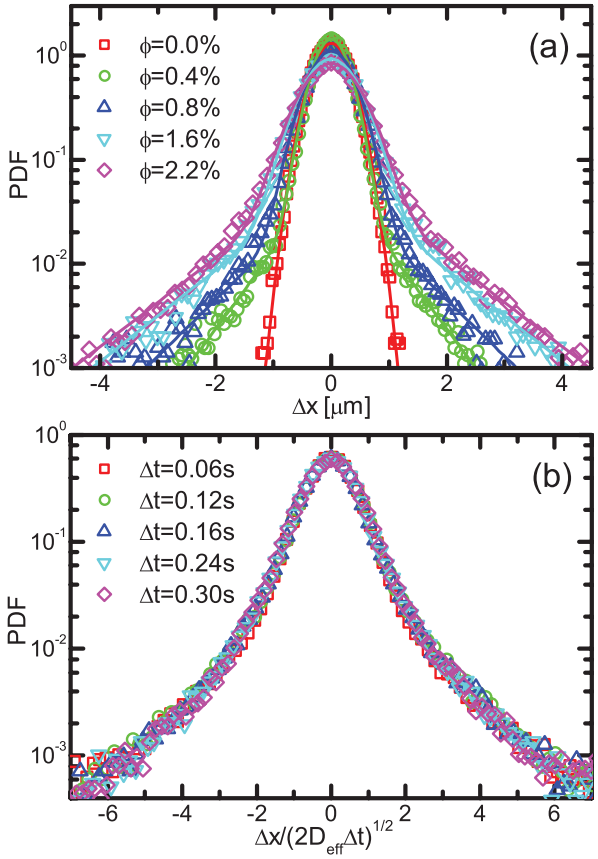

FIG. 2: (Color online) Probability distribution functions for tracer displacements. (a) Overlaid PDFs at a fixed time interval $\Delta t = 0.12$ s, for various volume fractions, showing the broadening of the Gaussian core and appearance of exponential tails. (b) Diffusive rescaling of PDFs at $\phi = 2.2\%$ and various time intervals, illustrating data collapse.

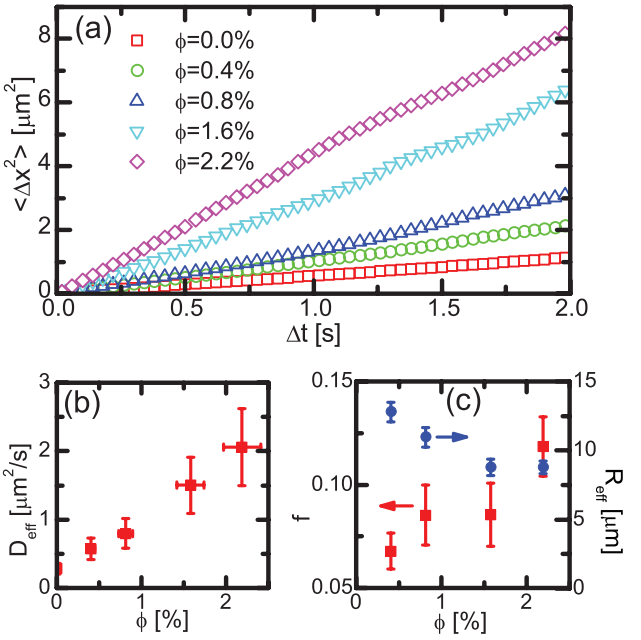

FIG. 3: (Color online) Diffusional characteristics. (a) Mean squared particle displacement at various cell concentrations. Concentration dependence of (b) effective diffusion coefficient and (c) fraction of PDF due to tails of the distribution (squares) and effective radius (circles).

implies that a diffusive rescaling of the displacements in terms of $\Delta x/(2D_{\rm eff}\Delta t)^{1/2}$ leads, at any given ϕ, to a data collapse, as shown in Fig. 2b, where $D_{\rm eff}$ is a constant (see below). Furthermore, despite the complex shape of the PDFs, the mean square displacement of the tracers remains quite linear in time, but with a slope that increases with ϕ, as shown in Fig. 3a. Similar trends have been seen in thin films of swimming bacteria [7]. We characterize this behavior by means of an effective diffusivity $D_{\rm eff} = \langle(\Delta x)^2\rangle/2\Delta t$. We find that $D_{\rm eff}$ varies smoothly with the volume fraction of swimmers with a form $D_{\rm eff} \simeq D_0 + \alpha\phi$, with $\alpha \sim 80$ μm^2/s (Fig. 3b). On dimensional grounds we expect $\alpha \sim U^2\tau \sim U\ell$, with U, τ, and ℓ a characteristic advective velocity, encounter time, and advected length. From Fig. 1c, a typical ℓ is seen to be $1-3$ μm, which implies $U \sim 30-80$ μm/s, quite consistent with the measured cell speed distribution (Fig. 1b). The value of f increases linearly with ϕ. This gives an estimate of the effective range $R_{\rm eff}$ over which advective contributions are substantial by the rescaling $f \simeq (R_{\rm eff}/R)^3\phi$. The values of $R_{\rm eff}$ are two to three times the cell radius and vary little with concentration.

These measurements suggest a heuristic picture of the suspension in which surrounding each swimming cell is a *sphere of influence* of radius $R_{\rm eff}$ within which advection strongly dominates diffusion, and outside of which tracers experience only thermal Brownian motion. This is consistent with the PDFs having the form of a weighted sum of the two distributions. The empirical $R_{\rm eff}$ and the fraction f provide measures of this sphere size; at the highest values $f \simeq 0.12$ the spheres occasionally overlap, like the random coils of a semidilute polymer solution.

A quantitative measure of the advection/diffusion balance comes from considering the flow field around a cell in the simplified form $u(r)\exp(i\omega t)$. Tracer oscillations are indistinguishable from Brownian motion at a radius $r_B > R_{\rm eff}$ where the displacement $2u(r_B)/\omega$ in a half cycle is comparable to the diffusive displacement $(2Dt)^{1/2}$ in a time $t = \pi/\omega$. For *Chlamydomonas* flagellar beating with $\omega = 2\pi \cdot 50$ rad/s this yields $u(r_B) \sim (2\pi D\omega)^{1/2} \sim 10$ μm/s, and a displacement ~ 0.1 μm. A direct experimental determination of r_B can be obtained from visualization of detailed tracer trajectories near free-swimming cells. Figure 4a shows one such trajectory, plotted in the frame of reference of the swimming *Chlamydomonas*, along with the time series of radial velocity in the laboratory frame. It is evident that the Brownian radius $r_B \simeq 25-30$ μm. For comparison one might ask when

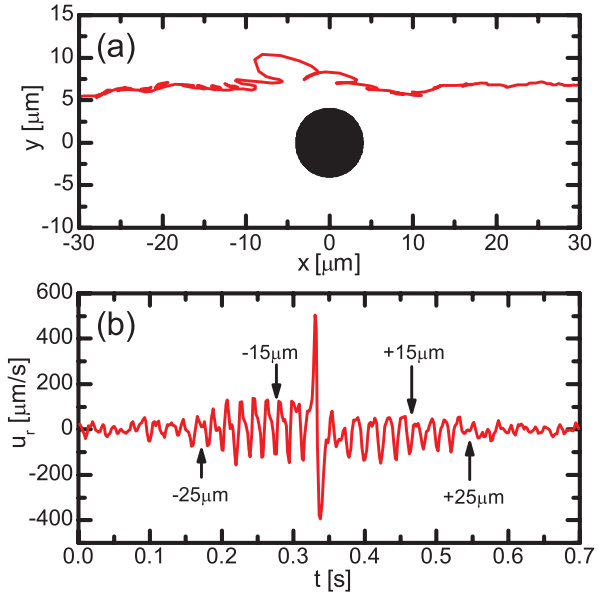

FIG. 4: (Color online) Tracer dynamics. (a) Trajectory of a tracer particle imaged at 500 fps, in a frame of reference moving with a *Chlamydomonas* cell. Black disk represents the approximate size of the cell. (b) Induced radial motion fades into Brownian motion beyond ~ 25 μm from the cell.

oscillatory displacements are comparable to the tracer radius, $2u(r_a)/\omega \simeq a$, which yields $u(r_a) \sim 150$ μm/s. Such velocities appear at distances of order 15 μm ($\sim R_{\rm eff}$). To go beyond these measurements to a model for the velocity field from which features such as r_B can be determined we note that the viscous penetration depth associated with the flagellar beating is $\xi = (2\nu/\omega)^{1/2} \simeq 80$ μm. The fact that this is only a few times larger than r_B implies that these flows are intrinsically *unsteady*; the far field is that of an unsteady stresslet [25]. Detailed comparison (discussed elsewhere) with tracer trajectories shows quantitative consistency with such models and confirms the length scale r_B. Moreover, the number of flagellar beats during the intervals Δt of the PDFs, and also during the encounter time of a tracer with a swimmer, can easily be ten or more. Such unsteadiness may be expected to alter significantly encounter rates in suspension feeding relative to those for steady flow [2, 3]. It also contributes to an enhanced tracer diffusivity, as in the problem of pollutant dispersal in oscillatory tidal flows, where techniques of Lagrangian averaging have proven useful [26].

We have shown that the statistics of passive tracers in suspensions of flagellated eukaryotes exhibits a non-Gaussian yet self-similar form, with clear systematics in the concentration of swimmers. Oscillatory components appear to play a significant role in the dynamics. Development of a statistical theory of the PDFs and the diffusional enhancement is clearly the main theoretical challenge. In closing we note that in contrast to bacteria, whose helical flagella push it through the fluid, *Chlamydomonas* is a "puller." Theoretical studies of instabilities in concentrated suspensions of swimmers [13, 15] suggest a profound difference between the two, with only pushers displaying large-scale coherence. The techniques outlined here may allow for sufficiently high concentrations of cells to test this prediction in detail.

We thank K. Drescher, B. Eckhardt, G.R. Grimmett, T.J. Pedley, and C.A. Solari for discussions, and N. Damean, D. Page-Croft and N. Price for technical assistance. This work was supported by the BBSRC, a Leverhulme Trust Visiting Professorship (JPG), NSF Grant DMR0803153 (JSG & JPG), and the Schlumberger Chair Fund. JPG appreciates the hospitality of DAMTP during the course of this work.

[1] J. Shimeta, Limnol. Oceanogr. **38**, 456 (1993).
[2] S. Mayer, Bull. Math. Biol. **62**, 1035 (2000).
[3] V.J. Langlois, *et al.*, Aquat. Microb. Ecol. **54**, 35 (2009).
[4] S. Humphries, Proc. Natl. Acad. Sci. USA **106**, 7882 (2009).
[5] V. Magar, T. Goto, and T.J. Pedley, Q. J. Mech. Appl. Math. **56**, 65 (2003).
[6] M.B. Short, *et al.*, Proc. Natl. Acad. Sci. USA **103**, 8315 (2006).
[7] X.-L. Wu and A. Libchaber, Phys. Rev. Lett. **84**, 3017 (2000).
[8] G.V. Soni, *et al.*, Biophys. J. **84**, 2634 (2003).
[9] C. Dombrowski, *et al.*, Phys. Rev. Lett. **93**, 098103 (2004).
[10] D.T.N. Chen, *et al.*, Phys. Rev. Lett. **99**, 148302 (2007).
[11] M.J. Kim and K.S. Breuer, Phys. Fluids **16**, L78 (2004).
[12] N. Darnton, *et al.*, Biophys. J. **86**, 1863 (2004).
[13] Y. Hatwalne, et al., Phys. Rev. Lett. 92, 118101 (2004).
[14] J.P. Hernandez-Ortiz, C.G. Stoltz, and M.D. Graham, Phys. Rev. Lett. **95**, 204501 (2005).
[15] D. Saintillan and M.J. Shelley, Phys. Fluids **20**, 123304 (2008).
[16] P.T.Underhill, J.P. Hernandez-Ortiz, and M.D. Graham, Phys. Rev. Lett. **100**, 248101 (2008).
[17] L. Angelani, R. Di Leonardo, and G. Ruocco, Phys. Rev. Lett. **102**, 048104 (2009).
[18] Z. Warhaft, Annu. Rev. Fluid Mech. **32**, 203 (2000).
[19] E.H. Harris, *The Chlamydomonas Sourcebook*, Vol. 1 (Academic Press, Oxford, 2009).
[20] D.B. Weibel *et al.*, Proc. Natl. Acad. Sci. USA **102**, 11963 (2005).
[21] Concentrations were corrected for phototaxis effects from epifluorescent illumination using a calibration based on microsphere diffusivity obtained from brightfield illumination with no phototaxis.
[22] N.T. Ouellette, H. Xu, and E. Bodenschatz, Exp. Fluids **40**, 301 (2006).
[23] V.A. Vladimirov, *et al.*, J. Exp. Biol. **207**, 1203 (2004).
[24] M. Polin, *et al.*, Science, in press (2009).
[25] C. Pozrikidis, Phys. Fluids A **1**, 1508 (1989).
[26] M.S. Krol, SIAM J. Appl. Math. **51**, 1622 (1991).